

# Apolipoprotein CIII hyperactivates $\beta$ cell $\text{Ca}_v1$ channels through SR-BI/ $\beta 1$ integrin-dependent coactivation of PKA and Src

Yue Shi · Guang Yang · Jia Yu · Lina Yu · Ruth Westenbroek · William A. Catterall · Lisa Juntti-Berggren · Per-Olof Berggren · Shao-Nian Yang

Received: 18 February 2013 / Revised: 6 July 2013 / Accepted: 29 July 2013 / Published online: 15 August 2013  
© Springer Basel 2013

**Abstract** Apolipoprotein CIII (ApoCIII) not only serves as an inhibitor of triglyceride hydrolysis but also participates in diabetes-related pathological events such as hyperactivation of voltage-gated  $\text{Ca}^{2+}$  ( $\text{Ca}_v$ ) channels in the pancreatic  $\beta$  cell. However, nothing is known about the molecular mechanisms whereby ApoCIII hyperactivates  $\beta$  cell  $\text{Ca}_v$  channels. We now demonstrate that ApoCIII increased  $\text{Ca}_v1$  channel open probability and density. ApoCIII enhanced whole-cell  $\text{Ca}^{2+}$  currents and the  $\text{Ca}_v1$  channel blocker nimodipine completely abrogated this enhancement. The effect of ApoCIII was not influenced by individual inhibition of PKA, PKC, or Src. However, combined inhibition of PKA, PKC, and Src counteracted the effect of ApoCIII, similar results obtained by coinhibition of PKA and Src. Moreover, knockdown of  $\beta 1$  integrin or scavenger receptor class B type I (SR-BI) prevented

ApoCIII from hyperactivating  $\beta$  cell  $\text{Ca}_v$  channels. These data reveal that ApoCIII hyperactivates  $\beta$  cell  $\text{Ca}_v1$  channels through SR-BI/ $\beta 1$  integrin-dependent coactivation of PKA and Src.

**Keywords**  $\text{Ca}^{2+}$  channel · Integrin · Pancreatic  $\beta$  cell · Protein kinase · Scavenger receptor

## Abbreviations

ApoCIII Apolipoprotein CIII  
 $\text{Ca}_v$  Voltage-gated  $\text{Ca}^{2+}$   
SR-BI Scavenger receptor class B type I

## Introduction

Voltage-gated calcium ( $\text{Ca}_v$ ) channels are critical in pancreatic  $\beta$  cell physiology and pathophysiology [1, 2]. They not only take center stage in the regulation of insulin secretion but are also involved in  $\beta$  cell development, survival, and growth through the regulation of protein phosphorylation, gene expression, and the cell cycle [1, 2]. The function and density of  $\beta$  cell  $\text{Ca}_v$  channels are regulated by a wide range of mechanisms either shared by other cell types or specific to  $\beta$  cells, e.g., channel phosphorylation, interaction with other molecules, and glucose metabolism-derived signaling [1–3]. Dysfunctional  $\text{Ca}_v$  channels cause  $\beta$  cell malfunction and even death as manifested in the most common metabolic disorder diabetes mellitus [1, 2]. Indeed, a T-lymphocyte-mediated autoimmune attack plays a crucial role in  $\beta$  cell death in type 1 diabetes. In addition, exposure to type 1 diabetic serum results in unphysiological amounts of  $\text{Ca}^{2+}$  in the pancreatic  $\beta$  cell and consequent  $\text{Ca}^{2+}$ -dependent apoptosis. This is, at least in part, due to excessive  $\text{Ca}^{2+}$  influx through hyperactivated  $\text{Ca}_v$  channels

Yue Shi and Guang Yang have contributed equally to this work.

**Electronic supplementary material** The online version of this article (doi:10.1007/s00018-013-1442-x) contains supplementary material, which is available to authorized users.

Y. Shi · G. Yang · J. Yu · L. Yu · L. Juntti-Berggren · P.-O. Berggren (✉) · S.-N. Yang (✉)  
The Rolf Luft Research Center for Diabetes and Endocrinology,  
Karolinska Institutet, SE-171 76 Stockholm, Sweden  
e-mail: per-olof.berggren@ki.se

S.-N. Yang  
e-mail: shao-nian.yang@ki.se

G. Yang  
Jilin Academy of Traditional Chinese Medicine,  
Changchun 130021, China

R. Westenbroek · W. A. Catterall  
Department of Pharmacology, School of Medicine, University  
of Washington, Seattle, WA 98195-7280, USA

[4, 5]. Undoubtedly, this process aggravates the disease development on top of the autoimmune attack [1, 2].

It has been demonstrated that elevated apolipoprotein CIII (ApoCIII) acts as a diabetogenic serum factor to drive  $\beta$  cell destruction via hyperactivation of  $\beta$  cell  $\text{Ca}_v$  channels [5, 6]. Moreover, we have recently shown that in vivo suppression of ApoCIII delays the onset of diabetes in the BioBreeding rat, a rat model for human type 1 diabetes [7]. Normally, ApoCIII is a blood plasma component. It is synthesized predominantly in the liver and to a minor extent in the intestine. Liver and intestinal cells release this apolipoprotein into the blood where it is situated on the surface of chylomicrons, very-low-density lipoproteins (VLDLs) and high-density lipoproteins (HDLs) [8, 9]. ApoCIII is composed of 79 amino acid residues that form six amphiphilic  $\alpha$ -helices, each containing about ten residues. The three-dimensional NMR structure and dynamics of ApoCIII have been resolved when it complexes with sodium dodecyl sulfate micelles, mimicking its natural lipid-bound state. The six amphiphilic  $\alpha$ -helices assemble into a necklace-like chain wrapping around the sodium dodecyl sulfate micelle surface [8]. Dogmatically, ApoCIII serves as an effective inhibitor of triglyceride hydrolysis by inhibiting lipoprotein lipase and through interference with triglyceride-rich lipoproteins binding to the negatively charged cell surface where lipoprotein lipases and lipoprotein receptors reside [8, 9]. It impedes the selective uptake of cholesteryl esters from LDL and HDL by binding to the scavenger receptor class B type I (SR-BI), and hampers the endocytosis of cholesterol-rich LDL by prevention of apolipoprotein B binding to LDL receptors [10–12]. Elevated plasma ApoCIII concentration is a feature of dyslipidemia in obesity and observed in both type 1 and 2 diabetes [5, 13, 14], whereas a group of Ashkenazi Jews with reduced plasma ApoCIII concentration maintains cardiovascular health and greater insulin sensitivity with age and reaches exceptional longevity [15].

In addition to the dogmatic roles in lipid metabolism, ApoCIII is also a multifaceted player in cell signaling. It can bind to distinct cell surface receptors including SR-BI and uncharacterized binding sites relaying corresponding signals to their downstream effectors, e.g.,  $\beta$ 1 integrin, pertussis toxin-sensitive G proteins, NF- $\kappa$ B, and protein kinases [10, 16–18]. However, nothing is known about the molecular mechanisms whereby ApoCIII hyperactivates  $\beta$  cell  $\text{Ca}_v$  channels. In the present study, we demonstrate that ApoCIII upregulates  $\beta$  cell  $\text{Ca}_v$ 1 channels through SR-BI/ $\beta$ 1 integrin-dependent coactivation of PKA and Src kinase.

## Materials and methods

### Cell culture and treatments

Islets of Langerhans were isolated from adult male and female mice and dispersed into single islet cells [19]. RINm5F cells at about 70 % confluency were trypsinized. The resultant suspension of cells was seeded into Petri dishes or 12-well plates. The cells were cultivated in RPMI 1640 medium supplemented with 10 % fetal bovine serum, 2 mM L-glutamine, and 100 U/100  $\mu$ g/ml penicillin/streptomycin (Invitrogen, Carlsbad, CA, USA) and maintained at 37 °C in a humidified 5 %  $\text{CO}_2$  incubator [19]. They were grown overnight and then subjected to siRNA transfection. For patch-clamp analysis, cells underwent overnight treatment with ApoCIII, the PKA inhibitors H-89 (Calbiochem, La Jolla, CA, USA) and myristoylated PKI (14–22) (PKI, Sigma–Aldrich, St. Louis, MO, USA), the PKC inhibitor calphostin C (Calbiochem), the Src kinase inhibitor PP2 (Calbiochem) and the  $\text{Ca}_v$ 1 channel blocker nimodipine (Calbiochem) in RPMI medium at final concentrations of 20  $\mu$ g/ml, 0.5, 1, 0.1, 0.1, and 5  $\mu$ M, respectively. ApoCIII was dissolved in 0.1 % trifluoroacetic acid (TFA) to make a stock solution of 1 mg/ml, PKI was dissolved in water to prepare a stock solution of 0.5 mM, whereas H-89, calphostin C, PP2, and nimodipine were dissolved in dimethyl sulfoxide (DMSO) to form stock solutions of 5, 1, 1, and 10 mM, respectively. As vehicle controls, 0.002 % TFA and/or 0.03 % DMSO were used.

### siRNA design and transfection

Two pairs of 21-mer siRNA duplexes targeting the rat  $\beta$ 1 integrin ( $\beta$ 1 integrin siRNA #1, ID127971 and  $\beta$ 1 integrin siRNA #2, ID127972) and SR-BI (ID128929) were designed and chemically synthesized by Applied Biosystems/Ambion (Austin, TX, USA). Their sequences were subjected to BLAST search to ensure their specificity. Silencer Select Negative Control siRNA (4390843), not targeting any gene product, and Silencer Select GAPDH Positive Control siRNA (4390849), efficiently silencing GAPDH in human, mouse, and rat cells, were purchased from Applied Biosystems/Ambion (Austin, TX, USA). RINm5F cells were reversely transfected with Lipofectamine RNAiMAX. Briefly, negative control siRNA,  $\beta$ 1 integrin siRNA #1,  $\beta$ 1 integrin siRNA #2 or SR-BI siRNA was mixed with Lipofectamine RNAiMAX followed by 20-min incubation at room temperature. Subsequently, cells were added to the siRNA/Lipofectamine RNAiMAX mixtures followed by gentle agitation and kept at 37 °C in a humidified 5 %  $\text{CO}_2$  incubator. After 72 h, the transfected

cells were grown to about 70 % confluency and subjected to different treatments followed by immunoblot assay or electrophysiological analysis.

#### Semiquantitative RT-PCR

Total RNA was isolated from RINm5F cells using the RNeasy Micro Kit as recommended by the manufacturer (Qiagen, Valencia, CA, USA). RT-PCR primer pairs were synthesized by Sigma–Aldrich. The SR-BI primer pair consisted of the forward primer 5'-CAAGAAGCCAAGCTGTAGGG-3' and the reverse primer 5'-CCCAACAGGCTCTACTCAGC-3'. The GAPDH primer pair comprised the forward primer 5'-TAGACAAGATGGTGAAGG-3' and the reverse primer 5'-TCCTTGAGGCCATGTAG-3'; 500 ng of total RNA was reverse transcribed with SuperScript II Reverse Transcriptase (Invitrogen) and Oligo(dT)12–18 Primer (Invitrogen). Polymerase chain reaction was carried out using the Platinum Taq DNA Polymerase (Invitrogen). It underwent 90 s at 94 °C for completely denaturing templates and activating the Taq DNA Polymerase, followed by 29 cycles of denaturing at 94 °C for 30 s, annealing at 55 °C for 30 s and extension at 72 °C for 30 s, and ending with a final extension at 72 °C for 5 min. The amplified PCR products were detected by agarose gel electrophoresis and ethidium bromide staining.

#### SDS-PAGE and immunoblot analysis

RINm5F cells following different treatments were lysed in a lysis buffer (pH 7.5) consisting of 50 mM HEPES, 150 mM NaCl, 1 mM EGTA, 1 mM EDTA, 10 % glycerol, 1 % triton X-100, 1 mM PMSF and a protease inhibitor cocktail (Roche Diagnostics, Mannheim, Germany). The lysate was centrifuged at  $800 \times g$  for 10 min at 4 °C to remove cell debris and nuclei. The protein concentration of the resulting samples was determined with Bio-Rad protein assay reagent (Bio-Rad, Hercules, CA, USA). The samples were denatured by heating at 96 °C for 3 min in SDS sample buffer and then underwent sodium dodecyl sulfate–polyacrylamide gel electrophoresis (SDS-PAGE) and immunoblot analysis. Briefly, 50, 90, or 180  $\mu$ g of protein were separated in discontinuous gels consisting of a 4 % acrylamide stacking gel (pH 6.8) and an 8 % acrylamide separating gel (pH 8.8). The separated proteins were then electroblotted to hydrophobic polyvinylidene difluoride membrane (Hybond-P; GE Healthcare, Uppsala, Sweden). The blots were blocked by incubation for 1 h with 5 % non-fat milk powder in a washing buffer, containing 50 mM Tris(hydroxymethyl)aminomethane, 150 mM NaCl and 0.05 % Tween 20 (pH 7.5). They were then incubated overnight at 4 °C with affinity-purified rabbit polyclonal antibodies to  $\beta$ 1 integrin (1:500; Millipore, Billerica, MA,

USA), SR-BI (1:2,500; Novus, Cambridge, UK),  $\text{Ca}_v1.2$  (1:200) and  $\text{Ca}_v1.3$  (1:200), respectively, and for 1 h at room temperature with mouse monoclonal antibody to glyceraldehyde-3-phosphate dehydrogenase (GAPDH, 1:4000; Applied Biosystems/Ambion, Austin, TX, USA), respectively. After rinsing with the washing buffer, the blots were incubated with the secondary antibodies (either horseradish peroxidase-conjugated goat anti-rabbit IgG or horseradish peroxidase-conjugated goat anti-mouse IgG; 1:50,000; Bio-Rad) at room temperature for 45 min. The immunoreactive bands were visualized with the ECL plus Western blotting detection system (GE Healthcare, Uppsala, Sweden).

#### Electrophysiology

Mouse islet cells and RINm5F cells following different treatments were subjected to single-channel and whole-cell patch-clamp measurements [20]. Cell-attached and perforated whole-cell patch-clamp configurations were employed [20]. Electrodes were made from borosilicate glass capillaries, fire-polished and coated with Sylgard close to their tips. Some of them were filled with a solution containing (in mM) 110  $\text{BaCl}_2$ , 10 TEA-Cl, and 5 HEPES [pH 7.4 with  $\text{Ba}(\text{OH})_2$ ] for single-channel measurements. Others were filled with a solution composed of (in mM) 76  $\text{Cs}_2\text{SO}_4$ , 1  $\text{MgCl}_2$ , 10 KCl, 10 NaCl, and 5 HEPES (pH 7.35 with CsOH), as well as amphotericin B (0.24 mg/ml) for whole-cell current recordings. Electrode resistance ranged between 4 and 6 M $\Omega$  when they were filled with electrode solutions and immersed in bath solutions. The electrode offset potential was corrected in bath solutions prior to gigaseal formation. Single-channel recordings were performed with cells bathed in a depolarizing external recording solution, containing (in mM) 125 KCl, 30 KOH, 10 EGTA, 2  $\text{CaCl}_2$ , 1  $\text{MgCl}_2$ , and 5 HEPES–KOH (pH 7.15). This solution was used to bring the intracellular potential to 0 mV. For perforated whole-cell current measurements, the cells were bathed in a solution containing (in mM) 138 NaCl, 5.6 KCl, 1.2  $\text{MgCl}_2$ , 10  $\text{CaCl}_2$ , 5 HEPES (pH 7.4). Single-channel and whole-cell currents were recorded with an Axopatch 200B amplifier (Molecular Devices, Foster City, CA, USA) and an EPC-9 patch clamp amplifier (HEKA Elektronik, Lambrecht/Pfalz, Germany), respectively, at room temperature (about 22 °C). Acquisition and analysis of single channel and whole-cell current data were done using the software program pCLAMP 10 (Axon Instruments) and the software program PatchMaster/FitMaster (HEKA), respectively. To guarantee elimination of rapid transient  $\text{Na}^+$  currents appearing at the initial period of depolarization during whole-cell  $\text{Ca}^{2+}$  current recordings [21], we measured peak whole-cell  $\text{Ca}^{2+}$  currents within a time window from 30 to 100 ms after the

start point of depolarization. The amplitude of whole-cell currents was normalized by the cell capacitance.

### Statistical analysis

All data are presented as mean  $\pm$  SEM. Statistical significance was determined by one-way ANOVA, followed by least significant difference (LSD) test. When two groups were compared, unpaired Student's *t* test or Mann–Whitney *U* test was employed. The significance level was set to 0.05 or 0.01.

## Results

### Apolipoprotein CIII increases $\text{Ca}_v1$ channel density and conductivity in the $\beta$ cell

Our previous work reveals that ApoCIII incubation significantly enhances whole-cell  $\text{Ca}^{2+}$  currents in the mouse islet  $\beta$  cell [5]. To clarify what type of  $\beta$  cell  $\text{Ca}_v$  channels and whether the density or conductivity was affected, we analyzed unitary  $\text{Ca}_v1$  channel currents, characterized by a large unitary  $\text{Ba}^{2+}$  conductance with long-lasting openings, in mouse islet  $\beta$  cells (Fig. 1a) and RINm5F cells (Fig. 1c), following ApoCIII incubation. In experiments with mouse islet  $\beta$  cells, we observed more  $\text{Ca}_v1$  channels, reflected by more layers of unitary  $\text{Ba}^{2+}$  currents, in plasma membrane patches of ApoCIII-treated cells than in those of control cells (Fig. 1a). The average number, open probability, and mean open time of unitary  $\text{Ca}_v1$  channels in ApoCIII-treated cells ( $n = 32$ ) were significantly greater than those in cells exposed to control vehicle ( $n = 33$ ); (Fig. 1b). The mean closed time of unitary  $\text{Ca}_v1$  channels recorded in patches of ApoCIII-incubated cells was significantly shorter than that in control patches (Fig. 1b). There is no significant difference in the unitary slope conductance of  $\text{Ca}_v1$  channels between control and ApoCIII treated groups ( $23.72 \pm 1.53$  versus  $23.87 \pm 1.42$  pS,  $p > 0.05$ ). Likewise, similar effects of ApoCIII occurred on  $\text{Ca}_v1$  channels in insulin-secreting RINm5F cells. Plasma membrane patches of ApoCIII-incubated cells accommodated more  $\text{Ca}_v1$  channels in comparison with those of vehicle-treated cells (Fig. 1c).  $\text{Ca}_v1$  channels in the former opened more frequently than those in the latter (Fig. 1c). ApoCIII incubation ( $n = 35$ ) significantly increased channel number, elevated open probability, prolonged mean open time and shortened mean closed time of  $\text{Ca}_v1$  channels as compared with incubation with vehicle solution ( $n = 34$ ) (Fig. 1d). However, it did not alter the unitary slope conductance of  $\text{Ca}_v1$  channels (control group:  $23.81 \pm 1.42$  pS versus ApoCIII group:  $24.15 \pm 1.07$  pS,  $p > 0.05$ ). Obviously, the data reveal that

ApoCIII increases both density and conductivity of  $\beta$  cell  $\text{Ca}_v1$  channels.

### Pharmacological ablation of $\text{Ca}_v1$ channels prevents apolipoprotein CIII-induced hyperactivation of $\beta$ cell $\text{Ca}_v$ channels

The verification of the effects of ApoCIII on  $\text{Ca}_v1$  channels by single-channel analysis does not necessarily mean that ApoCIII only affects  $\text{Ca}_v1$  channels. To examine if the effects also occur on other types of  $\text{Ca}_v$  channels, we analyzed whole-cell  $\text{Ca}^{2+}$  currents in RINm5F cells following ApoCIII incubation in the absence and presence of the  $\text{Ca}_v1$  channel blocker nimodipine. Whole-cell  $\text{Ca}^{2+}$  currents in cells incubated with ApoCIII were larger than those in cells treated with vehicle solution (Fig. 2a). Whole-cell  $\text{Ca}^{2+}$  current densities observed in the voltage range from 10 to 30 mV in the ApoCIII group were significantly higher than those in the control group (Fig. 2b). In striking contrast, whole-cell  $\text{Ca}^{2+}$  currents were similar between control cells and cells incubated with ApoCIII in the presence of nimodipine (Fig. 2c). There was no significant difference in the whole-cell  $\text{Ca}^{2+}$  current density between the two treatments (Fig. 2d). The data confirm that ApoCIII solely impinges on  $\beta$  cell  $\text{Ca}_v1$  channels.

### Apolipoprotein CIII hyperactivates $\beta$ cell $\text{Ca}_v$ channels via coactivation of PKA and Src kinase

The increase in open probability of  $\beta$  cell  $\text{Ca}_v1$  channels by ApoCIII and the mediating role of protein kinases in ApoCIII signaling suggest that ApoCIII may signal upstream of some protein kinases to hyperactivate  $\beta$  cell  $\text{Ca}_v$  channels [16, 22–25]. Therefore, we explored the involvement of PKA, PKC, and Src kinase in ApoCIII-induced hyperactivation of  $\beta$  cell  $\text{Ca}_v$  channels.

First, we examined the effect of the PKA inhibitor H-89 on ApoCIII-induced hyperactivation of  $\beta$  cell  $\text{Ca}_v$  channels in RINm5F cells. Whole-cell  $\text{Ca}^{2+}$  currents registered in control cells were smaller than those in cells treated with ApoCIII, whereas whole-cell  $\text{Ca}^{2+}$  currents recorded in cells incubated with ApoCIII plus H-89 sized in between (Fig. 3a). Average  $\text{Ca}^{2+}$  current densities measured in ApoCIII-treated cells (filled circles,  $n = 36$ ) were significantly higher than those in vehicle-treated control cells (open circles,  $n = 37$ ) at voltages ranging from 10 to 50 mV (Fig. 3b). However, cells following cotreatment of ApoCIII and H-89 (filled triangles,  $n = 36$ ) did not significantly differ from either cells treated with ApoCIII or control cells in terms of  $\text{Ca}^{2+}$  current density (Fig. 3b). Moreover, H-89 treatment did not significantly influence  $\text{Ca}^{2+}$  current densities under basal conditions, i.e., in the absence of ApoCIII (Supplementary Fig. S1A and B). In addition, we

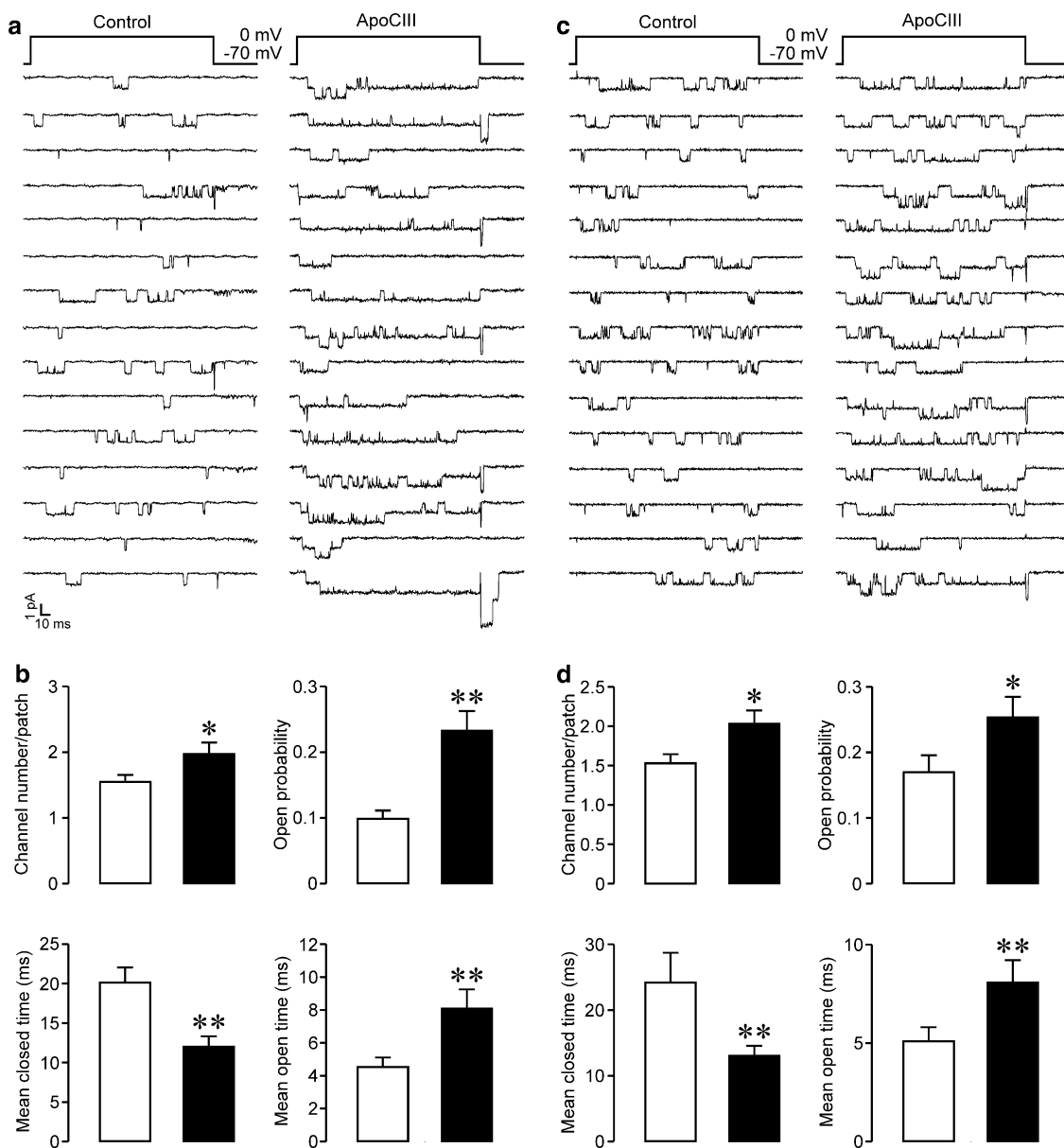


**Fig. 1** Apolipoprotein CIII incubation increases both the density and conductivity of  $\text{Ca}_v1$  channels in  $\beta$  cells. **a** Examples of unitary  $\text{Ca}_v1$  channel currents detected in plasma membrane patches of mouse islet  $\beta$  cells incubated with either vehicle solution as control or apolipoprotein CIII (ApoCIII). **b** Average number, open probability, mean closed time, and mean open time of unitary  $\text{Ca}_v1$  channels measured in plasma membrane patches attached to mouse islet  $\beta$  cells exposed to either control vehicle (open columns,  $n = 33$ ) or ApoCIII (filled col-

umns,  $n = 32$ ). **c** Examples of unitary  $\text{Ca}_v1$  channel currents recorded in plasma membrane patches attached to either a control RINm5F cell or a cell treated with ApoCIII. **d** Average number, open probability, mean closed time, and mean open time of unitary  $\text{Ca}_v1$  channels detected in plasma membrane patches of control RINm5F cells (open columns,  $n = 34$ ) or cells incubated with ApoCIII (filled columns,  $n = 35$ ). \* $p < 0.05$  and \*\* $p < 0.01$  versus control

also evaluated the effect of the more specific PKA inhibitor myristoylated PKI on ApoCIII-induced hyperactivation of  $\beta$  cell  $\text{Ca}_v$  channels since H-89 might produce non-specific effects. Figure 4 shows that whole-cell  $\text{Ca}^{2+}$  currents observed in cells exposed to ApoCIII (open circles,  $n = 30$ ) were significantly greater than those in cells treated with vehicle solution (filled circles,  $n = 30$ ). Whole-cell  $\text{Ca}^{2+}$

currents recorded in ApoCIII-treated cells in the presence of PKI (filled triangles,  $n = 30$ ) fell between the former and the latter (Fig. 4). Furthermore, PKI treatment had no effect on whole-cell  $\text{Ca}^{2+}$  currents in the absence of ApoCIII (Supplementary Fig. S3). The results indicate that PKA inhibition marginally reduces ApoCIII-induced hyperactivation of  $\beta$  cell  $\text{Ca}_v$  channels.

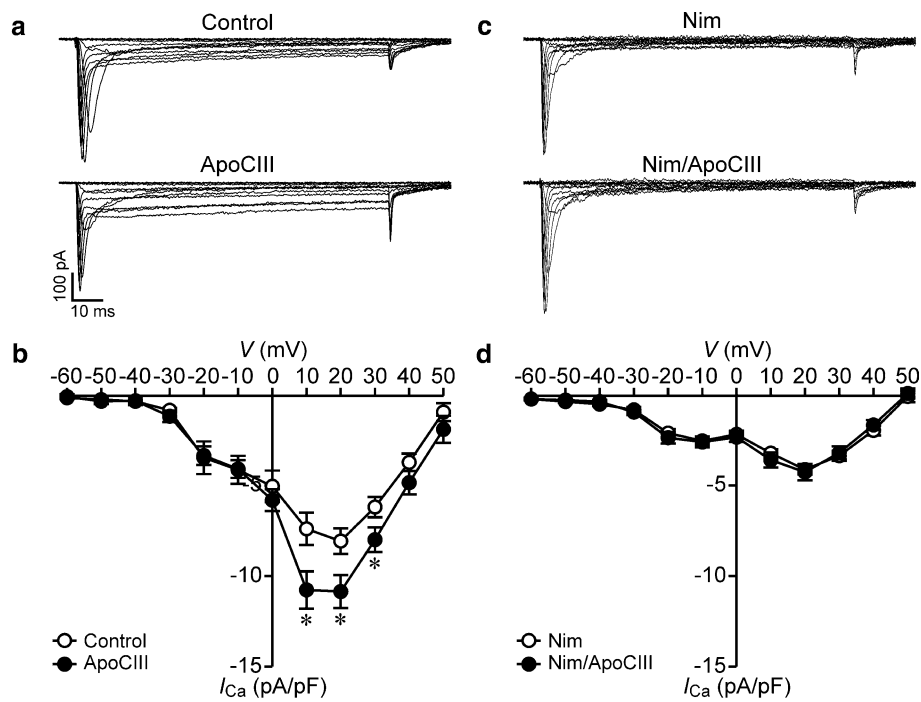


**Fig. 2** Apolipoprotein CIII incubation increases whole-cell  $\text{Ca}^{2+}$  currents and coincubation with the  $\text{Ca}_v1$  channel blocker nimodipine abrogates the effect of apolipoprotein CIII incubation in RINm5F cells. **a** Sample whole-cell  $\text{Ca}^{2+}$  current traces from a cell incubated with vehicle solution as control (cell capacitance: 10.1 pF) and apolipoprotein CIII (ApoCIII)-treated cell (cell capacitance: 11.1 pF). **b** Average  $\text{Ca}^{2+}$  current density-voltage relationships in control cells

(open circles,  $n = 26$ ) and cells treated with ApoCIII (filled circles,  $n = 26$ ). \* $p < 0.05$  versus control. **c** Sample whole-cell  $\text{Ca}^{2+}$  current traces from a nimodipine (Nim)-incubated cell (cell capacitance: 10 pF) and a cell exposed to Nim together with ApoCIII (Nim/ApoCIII) (cell capacitance: 11.9 pF). **d** Average  $\text{Ca}^{2+}$  current density-voltage relationships in Nim-treated cells (open circles,  $n = 20$ ) and cells incubated with Nim/ApoCIII (filled circles,  $n = 21$ )

Second, we tested the effect of the PKC inhibitor calphostin C (CalpC) on ApoCIII-induced hyperactivation of  $\beta$  cell  $\text{Ca}_v$  channels in RINm5F cells. We observed that cells incubated with ApoCIII and ApoCIII/CalpC-cotreated cells displayed similar whole-cell  $\text{Ca}^{2+}$  currents, which were larger than those acquired in vehicle-treated cells (Fig. 3c). Mean  $\text{Ca}^{2+}$  current densities in ApoCIII-treated cells (filled circles,  $n = 33$ ) at the voltage range of 10–50 mV and cells exposed to ApoCIII/CalpC (filled triangles,  $n = 33$ ) at a voltage range from 20 to 50 mV increased significantly in comparison with vehicle-treated control cells (open circles,  $n = 33$ ) (Fig. 3d). There is no difference between ApoCIII-treated cells and ApoCIII/CalpC-cotreated cells with regard to the  $\text{Ca}^{2+}$  current density (Fig. 3d). Furthermore, cells exposed to control vehicle were similar to CalpC-treated cells in terms of  $\text{Ca}^{2+}$  current density (Supplementary Fig. S1C and D). These data demonstrate that PKC inhibition does not affect ApoCIII-induced hyperactivation of  $\beta$  cell  $\text{Ca}_v$  channels.

Third, we evaluated the effect of the Src kinase inhibitor PP2 on ApoCIII-induced hyperactivation of  $\beta$  cell  $\text{Ca}_v$  channels in RINm5F cells. We found smaller and larger whole-cell  $\text{Ca}^{2+}$  currents in cells following

incubation with vehicle solution and ApoCIII-incubated cells, respectively (Fig. 3e). Cells exposed to ApoCIII and PP2 fell between vehicle control cells and cells treated with ApoCIII with regard to whole-cell  $\text{Ca}^{2+}$  currents (Fig. 3e). Whole-cell  $\text{Ca}^{2+}$  current densities quantified in cells treated with ApoCIII (filled circles,  $n = 40$ ) at the voltage range 10–50 mV were significantly elevated as compared with those determined in vehicle control cells (open circles,  $n = 40$ ); (Fig. 3f). Cells subjected to cotreatment of ApoCIII and PP2 (filled triangles,  $n = 40$ ) showed significantly larger  $\text{Ca}^{2+}$  currents at the voltage range 20–40 mV compared to vehicle-treated control cells (open circles,  $n = 40$ ). However, the difference in the  $\text{Ca}^{2+}$  current density between ApoCIII/PP2-cotreated cells and cells incubated with vehicle solution is less prominent than that between cells treated with ApoCIII and vehicle-treated control cells (Fig. 3f). Moreover, vehicle-treated cells (open circles,  $n = 20$ ) and cells incubated with PP2 (filled circles,  $n = 19$ ) exhibited similar  $\text{Ca}^{2+}$  current densities (Supplementary Fig. S1E and F). The results suggest that Src kinase inhibition has a tendency to decrease ApoCIII-induced hyperactivation of  $\beta$  cell  $\text{Ca}_v$  channels.

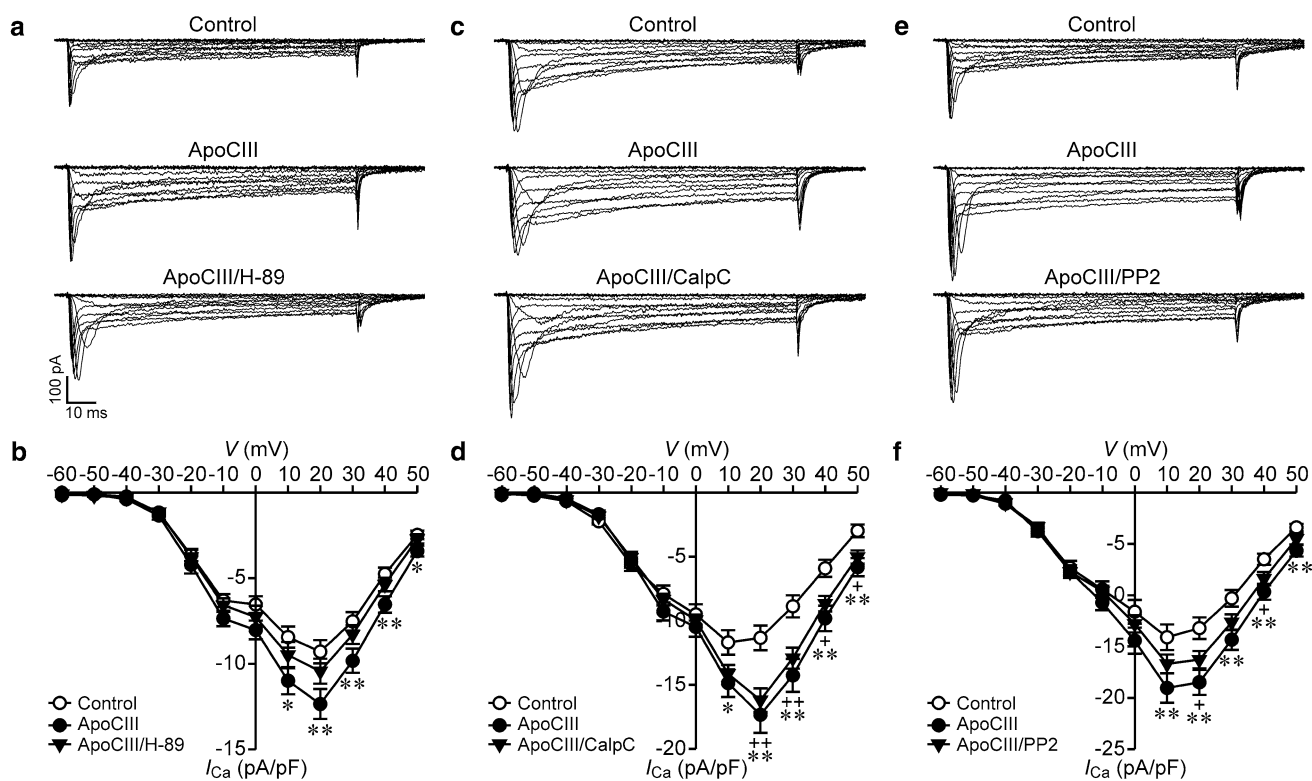


**Fig. 3** PKA or Src kinase inhibition marginally reduces but PKC inhibition does not affect apolipoprotein CIII-induced enhancement of whole-cell  $\text{Ca}^{2+}$  currents in RINm5F cells. **a** Sample whole-cell  $\text{Ca}^{2+}$  current traces from a cell incubated with vehicle solution as control (cell capacitance: 8.5 pF), an apolipoprotein CIII (ApoCIII)-treated cell (cell capacitance: 8.2 pF) and a cell exposed to ApoCIII plus the PKA inhibitor H-89 (ApoCIII/H-89, cell capacitance: 8.4 pF). **b** Average  $\text{Ca}^{2+}$  current density–voltage relationships in control cells (open circles,  $n = 37$ ) and cells treated with ApoCIII (filled circles,  $n = 36$ ) or ApoCIII/H-89 (filled triangles,  $n = 36$ ). \* $p < 0.05$  and \*\* $p < 0.01$  versus control. **c** Sample whole-cell  $\text{Ca}^{2+}$  current traces registered in a control cell (cell capacitance: 12.5 pF), an ApoCIII-incubated cell (cell capacitance: 12.0 pF) and a cell subjected to cotreatment with ApoCIII and the PKC inhibitor calphostin C (ApoCIII/CalpC, cell

capacitance: 12.1 pF). **d** Average  $\text{Ca}^{2+}$  current density–voltage relationships in control cells (open circles,  $n = 33$ ), ApoCIII-treated cells (filled circles,  $n = 33$ ) and cells exposed to ApoCIII/CalpC (filled triangles,  $n = 33$ ). \* $p < 0.05$  and \*\* $p < 0.01$  ApoCIII versus control. + $p < 0.05$  and ++ $p < 0.01$  ApoCIII/CalpC versus control. **e** Sample whole-cell  $\text{Ca}^{2+}$  current traces acquired in a control cell (cell capacitance: 9.5 pF), an ApoCIII-incubated cell (cell capacitance: 9.2 pF) and a cell exposed to ApoCIII together with the Src kinase inhibitor PP2 (ApoCIII/PP2, cell capacitance: 10.0 pF). **f** Average  $\text{Ca}^{2+}$  current density–voltage relationships in control cells (open circles,  $n = 40$ ) and cells incubated with ApoCIII (filled circles,  $n = 40$ ) or ApoCIII/PP2 (filled triangles,  $n = 40$ ). \*\* $p < 0.01$  ApoCIII versus control. + $p < 0.05$  ApoCIII/PP2 versus control

The marginal and null effects of PKA, PKC or Src kinase inhibitors on ApoCIII-induced hyperactivation of  $\beta$  cell  $\text{Ca}_v$  channels made us wonder what happens if a more complex inhibition of all these kinases is applied. To address this question, we characterized the effect of the protein kinase inhibitor cocktail H-89, CalpC and PP2 on ApoCIII-induced hyperactivation of  $\beta$  cell  $\text{Ca}_v$  channels in RINm5F cells. Larger whole-cell  $\text{Ca}^{2+}$  currents appeared in an ApoCIII-treated cells, whereas smaller whole-cell  $\text{Ca}^{2+}$  currents occurred in vehicle-treated control cells and cells treated with ApoCIII in the presence of H-89, CalpC and PP2 (Fig. 5a). ApoCIII treatment (filled circles,  $n = 35$ ) significantly increased  $\text{Ca}^{2+}$  current densities at the voltage range 10–40 mV as compared with vehicle-treated control cells (open circles,  $n = 35$ ) and treatment with

ApoCIII together with H-89, CalpC and PP2 (filled triangles,  $n = 34$ ). The profile of  $\text{Ca}^{2+}$  current densities in cells exposed to ApoCIII in the presence of H-89, CalpC and PP2 resembled that in vehicle-treated control cells (Fig. 5b). Furthermore, treatment of control cells with the protein kinase inhibitor cocktail H-89, CalpC and PP2 had no significant effect on whole-cell  $\text{Ca}^{2+}$  currents under basal conditions, i.e., in the absence of ApoCIII (Supplementary Fig. S2A and B). H-89 might produce non-specific effects. To exclude this, we performed another set of experiments where PKI substituted for H-89. The data obtained with PKI were similar to those with H-89 (Fig. 4 and Supplementary Fig. S3). The results demonstrate that combined inhibition of PKA, PKC and Src kinase effectively ablates ApoCIII-induced hyperactivation of  $\beta$  cell  $\text{Ca}_v$  channels.

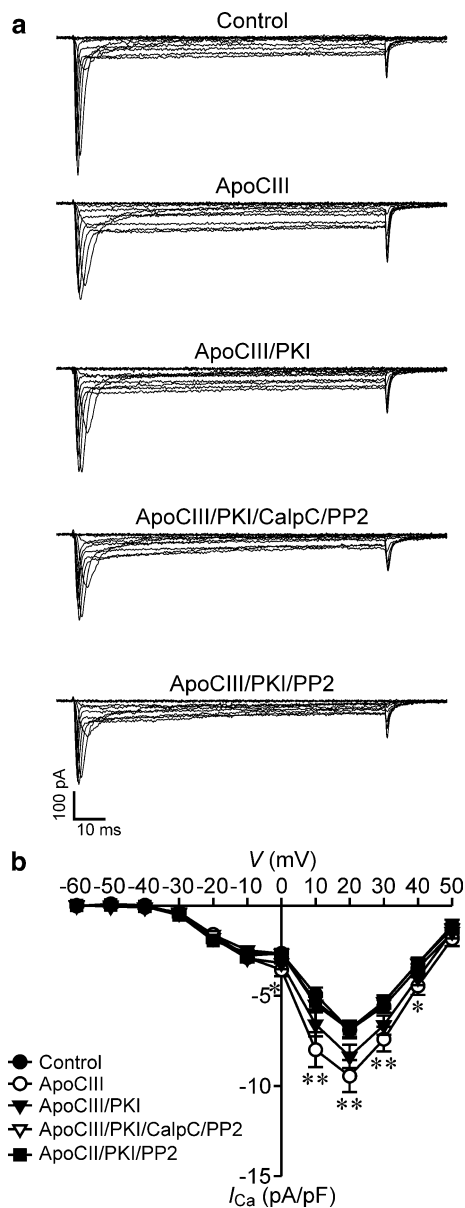


**Fig. 4** PKI alone marginally diminishes, but PKI in combination with either dual inhibition of PKC and Src kinase or singular inhibition of Src kinase ablates apolipoprotein CIII-induced elevation of whole-cell  $\text{Ca}^{2+}$  currents in RINm5F cells. **a** Sample whole-cell  $\text{Ca}^{2+}$  current traces acquired in a vehicle-incubated cell (control, cell capacitance: 12.03 pF), a cell treated with apolipoprotein CIII (ApoCIII, cell capacitance: 12.08 pF), a cell subsequent to co-treatment with ApoCIII and PKI (ApoCIII/PKI, cell capacitance: 12.5 pF), a cell exposed to ApoCIII in the presence of the protein kinase inhibitor cocktail of PKI, calphostin C and PP2 (ApoCIII/PKI/CalpC/PP2, cell capacitance: 12.27 pF) and a cell incubated with ApoCIII together with PKI and PP2 (ApoCIII/PKI/PP2, cell capacitance: 12.6 pF). **b** Average  $\text{Ca}^{2+}$  current density–voltage relationships in control cells (filled circles,  $n = 30$ ), cells treated with ApoCIII (open circles,  $n = 30$ ), cells incubated with ApoCIII/PKI (filled triangles,  $n = 30$ ) and cells exposed to ApoCIII/PKI/CalpC/PP2 (open triangles,  $n = 30$ ), or to ApoCIII/PKI/PP2 (filled squares,  $n = 30$ ). \* $p < 0.05$  and \*\* $p < 0.01$  versus control, ApoCIII/PKI/CalpC/PP2 and ApoCIII/PKI/PP2

The marginal effect of PKA or Src kinase inhibitors alone on whole-cell  $\text{Ca}^{2+}$  currents inevitably raised the question if coinhibition of PKA and Src kinase is sufficient to prevent ApoCIII-induced hyperactivation of  $\beta$  cell  $\text{Ca}_V$  channels. We answered the question by analyzing whole-cell  $\text{Ca}^{2+}$  currents in RINm5F cells following cotreatment with H-89 and PP2. We observed that whole-cell  $\text{Ca}^{2+}$  currents in ApoCIII-treated cells were larger than those in control cells or cells subjected to treatment with ApoCIII in the presence of H-89 and PP2 (Fig. 5c). Significantly higher densities of whole-cell  $\text{Ca}^{2+}$  currents appeared in the ApoCIII group (filled circles,  $n = 26$ ) in comparison with control group (open circles,  $n = 26$ ) or the group subjected to incubation with ApoCIII in the presence of H-89 and PP2 (filled triangles,  $n = 27$ ); (Fig. 5d). Moreover, whole-cell  $\text{Ca}^{2+}$  currents in control cells resembled those observed in cells treated with H-89 and PP2 (Supplementary Fig. S2C and D). To rule out the possibility of non-specific effects of H-89, we replaced H-89 with PKI. In fact, PKI produced similar results to those above-described in the presence of H-89 (Fig. 4; Supplementary Fig. S3). These data reveal that ApoCIII enhances whole-cell  $\text{Ca}^{2+}$  currents via coactivation of PKA and Src Kinase.

Apolipoprotein CIII does not influence  $\beta$  cell  $\text{Ca}_V1$  channel expression

Overnight incubation with ApoCIII may influence  $\beta$  cell  $\text{Ca}_V1$  channel expression. To test for this possibility, we analyzed  $\beta$  cell  $\text{Ca}_V1$  channel expression in RINm5F cells following ApoCIII incubation. We found that anti- $\text{Ca}_V1.2$ , anti- $\text{Ca}_V1.3$  and anti-GAPDH antibodies detected clear  $\text{Ca}_V1.2$ ,  $\text{Ca}_V1.3$  and GAPDH immunoreactive bands, respectively. Control and ApoCIII-treated samples gave similar intensities of  $\text{Ca}_V1.2$ ,  $\text{Ca}_V1.3$  and GAPDH immunoreactivities (Fig. 6a). Figure 6b shows that there was no significant difference in the relative abundance of  $\text{Ca}_V1.2$  (hatched column,  $n = 6$ ) and  $\text{Ca}_V1.3$  subunits (filled column,  $n = 6$ ) in RINm5F cell homogenates subjected to ApoCIII incubation in comparison with vehicle incubation (open column,  $n = 6$ ) ( $p > 0.05$ ). The data reveal that ApoCIII incubation does not alter  $\beta$  cell  $\text{Ca}_V1$  channel expression at the protein level.

Apolipoprotein CIII upregulates  $\beta$  cell  $\text{Ca}_V$  channels via  $\beta 1$  integrin

$\beta 1$  integrin has been verified to serve as a mediator between ApoCIII and a certain number of protein kinases including PKA and Src kinase [16, 22–25]. This together with our results that ApoCIII hyperactivated  $\beta$  cell  $\text{Ca}_V$  channels via coactivation of PKA and Src kinase raises the possibility



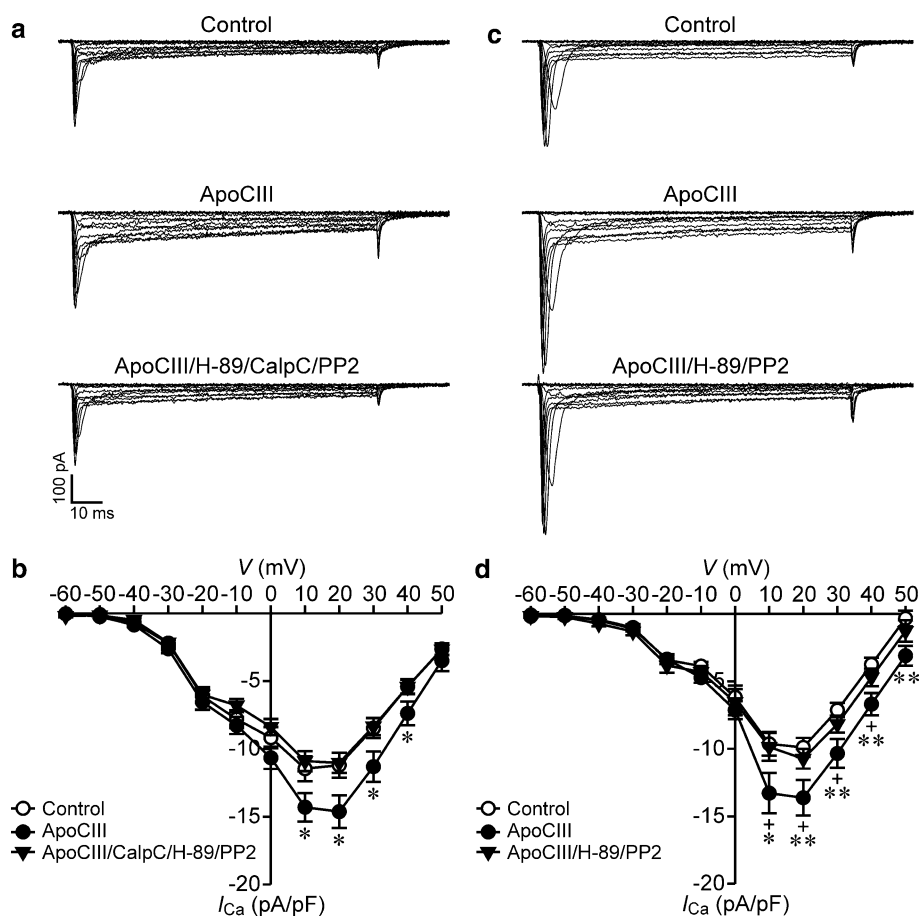


**Fig. 5** Combined inhibition of PKA, PKC, and Src kinase counteracts apolipoprotein CIII-induced augmentation of whole-cell  $Ca^{2+}$  currents in RINm5F cells and coinhibition of PKA and Src kinase is sufficient to obtain this counteraction. **a** Sample whole-cell  $Ca^{2+}$  current traces registered in a vehicle-incubated cell (Control, cell capacitance: 7.9 pF), a cell subsequent to apolipoprotein CIII (ApoCIII) treatment (cell capacitance: 7.0 pF) and a cell exposed to ApoCIII in the presence of the protein kinase inhibitor cocktail of H-89, calphostin C and PP2 (ApoCIII/H-89/CalpC/PP2, cell capacitance: 7.2 pF). **b** Average  $Ca^{2+}$  current density–voltage relationships in control cells (open circles,  $n = 35$ ) and cells exposed to ApoCIII (filled circles,  $n = 34$ )

or to ApoCIII/H-89/CalpC/PP2 (filled triangles,  $n = 35$ ).  $*p < 0.05$  versus control and apoCIII/H-89/CalpC/PP2. **c** Sample whole-cell  $Ca^{2+}$  current traces from a control cell (cell capacitance: 8.5 pF), a cell subsequent to ApoCIII treatment (cell capacitance: 8.2 pF) and a cell exposed to ApoCIII in the presence of the protein kinase inhibitors H-89 and PP2 (ApoCIII/H-89/PP2, cell capacitance: 8.7 pF). **d** Average  $Ca^{2+}$  current density–voltage relationships in control cells (open circles,  $n = 26$ ) and cells subjected to ApoCIII (filled circles,  $n = 26$ ) or to ApoCIII/H-89/PP2 (filled triangles,  $n = 27$ ).  $*p < 0.05$  and  $**p < 0.01$  versus control;  $+p < 0.05$  versus ApoCIII/H-89/PP2

that  $\beta 1$  integrin mediates ApoCIII-induced hyperactivation of  $\beta$  cell  $Ca_v$  channels. We investigated this possibility by implementing RNA interference in combination with whole-cell  $Ca^{2+}$  current analysis in RINm5F cells. It turned out that transfection with two  $\beta 1$  integrin siRNAs significantly decreased  $\beta 1$  integrin expression at the protein level (Fig. 7a, b). Importantly,  $\beta 1$  integrin siRNA pretransfection effectively prevented ApoCIII-induced hyperactivation of  $\beta$  cell  $Ca_v$  channels (Fig. 7c, d). Whole-cell  $Ca^{2+}$  currents in  $\beta 1$  integrin siRNA-pretransfected cells incubated with ApoCIII ( $\beta 1$  integrin siRNA/ApoCIII) were significantly smaller than those in negative control siRNA-pretransfected cells exposed to ApoCIII (NC siRNA/apoCIII), but similar to those in three sets of control cells (Fig. 7c).

These control cells were subjected to mock (NO siRNA/Control), negative control siRNA (NC siRNA/Control) and  $\beta 1$  integrin siRNA pretransfection ( $\beta 1$  integrin siRNA/Control), respectively, followed by control vehicle incubation (Fig. 7c). Significantly-reduced  $Ca^{2+}$  current density was observed in cells subsequent to  $\beta 1$  integrin siRNA/ApoCIII ( $n = 29$ ) in comparison with those to NC siRNA/apoCIII (filled triangles,  $n = 28$ ); (Fig. 7d). The former displayed similar  $Ca^{2+}$  current density, but the latter exhibited larger  $Ca^{2+}$  current density compared with those subjected to NO siRNA/Control ( $n = 29$ ), NC siRNA/Control ( $n = 28$ ) or  $\beta 1$  integrin siRNA/Control ( $n = 29$ ); (Fig. 7d). Taken together, the results demonstrate that ApoCIII critically relies on  $\beta 1$  integrin to hyperactivate  $\beta$  cell  $Ca_v$  channels.

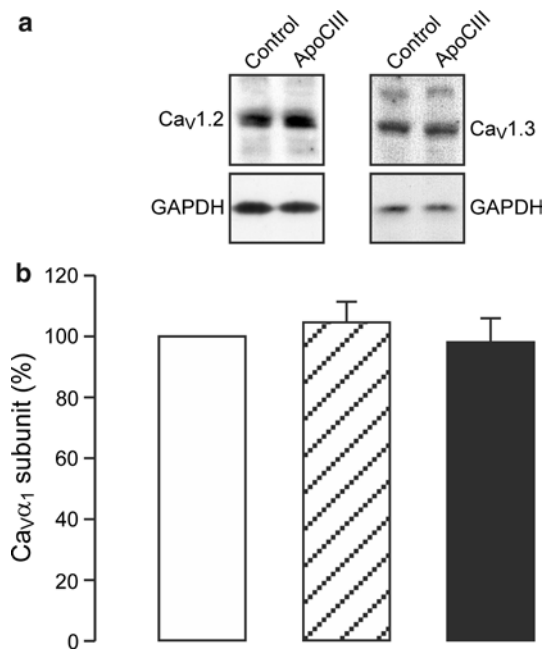


**Fig. 6** Apolipoprotein CIII incubation does not alter  $\beta$  cell  $\text{Ca}_V1$  channel expression. **a** Representative immunoblots of RINm5F cell homogenates, subjected to incubation with vehicle as control or apolipoprotein CIII (ApoCIII), probed with anti- $\text{Ca}_V1.2$ , anti- $\text{Ca}_V1.3$  and anti-GAPDH antibodies, respectively. **b** Immunoblot quantification of the relative abundance of  $\text{Ca}_V1.2$  (hatched column,  $n = 6$ ) and  $\text{Ca}_V1.3$  subunits (filled column,  $n = 6$ ) in RINm5F cell homogenates subjected to ApoCIII incubation in comparison with control (open column,  $n = 6$ ). There was no significant difference in the relative abundance of total  $\text{Ca}_V1.2$  and  $\text{Ca}_V1.3$  subunits between control cells and cells incubated with ApoCIII ( $p > 0.05$ )

#### Apolipoprotein CIII hyperactivates $\beta$ cell $\text{Ca}_V$ channels via SR-BI

Previous studies have shown that there is no direct interaction of ApoCIII with  $\beta 1$  integrin [16, 18]. In search for a molecular bridge between ApoCIII and  $\beta 1$  integrin we focused our interest to SR-BI since this receptor physically associates with ApoCIII and interacts with  $\beta 1$  integrin [10, 26]. We combined siRNA-mediated gene silencing and whole-cell  $\text{Ca}^{2+}$  current analysis to examine if SR-BI can serve as a molecular bridge between ApoCIII and  $\beta 1$  integrin in hyperactivating  $\beta$  cell  $\text{Ca}_V1$  channels. As shown in Fig. 8a–d, SR-BI siRNA transfection significantly lowered SR-BI at both mRNA and protein levels in RINm5F cells. It is important to note that such down-regulation sufficiently abolished enhancement of whole-cell  $\text{Ca}^{2+}$  currents by ApoCIII (Fig. 8e, f). Figure 8e shows that SR-BI siRNA pretransfected cells incubated with ApoCIII (SR-BI siRNA/ApoCIII) exhibited smaller whole-cell  $\text{Ca}^{2+}$  currents as compared with those pretransfected with negative control siRNA followed by ApoCIII exposure (NC siRNA/apoCIII). Whole-cell  $\text{Ca}^{2+}$  currents

in cells subjected to SR-BI siRNA/ApoCIII did not differ from those in control vehicle-treated cells subjected to mock (NO siRNA/Control), negative control siRNA (NC siRNA/Control) and SR-BI siRNA pretransfection (SR-BI siRNA/Control), respectively (Fig. 8e). In contrast, whole-cell  $\text{Ca}^{2+}$  currents in NC siRNA/apoCIII-treated cells were larger than those visualized in the aforementioned control cells (Fig. 8e).  $\text{Ca}^{2+}$  current density in SR-BI siRNA/ApoCIII group ( $n = 30$ ) was significantly decreased in comparison with that in NC siRNA/apoCIII group (filled triangles,  $n = 30$ ); (Fig. 8f). The former is similar to, but the latter is significantly larger than that in NO siRNA/Control ( $n = 30$ ), NC siRNA/Control ( $n = 29$ ) or SR-BI siRNA/Control ( $n = 29$ ); (Fig. 8f). The data verify that ApoCIII employs SR-BI as an indispensable conveyor for signaling from this apolipoprotein to  $\beta$  cell  $\text{Ca}_V$  channels.

#### Discussion

The gross conductivity of  $\text{Ca}_V$  channels depends on the density and activity of functional channels in the plasma membrane of the cell. Enhancement of whole-cell  $\text{Ca}^{2+}$  currents by type 1 diabetic serum and its factor ApoCIII can result from enriched density and/or increased conductivity of functional  $\text{Ca}_V$  channels in the  $\beta$  cell plasma membrane [4, 5]. However, all studies [1, 2, 5, 27] except one [4] have so far examined the effect of type 1 diabetic serum on  $\text{Ca}_V$  channels only at the whole cell level. In the study by Juntti-Berggren et al. [4] the increase in  $\beta$  cell  $\text{Ca}_V$  channel activity by type 1 diabetic serum was characterized at both the single channel and the whole-cell level. However, this work did not analyze whether type 1 diabetic serum could alter the density of functional  $\text{Ca}_V$  channels in the  $\beta$  cell plasma membrane [4]. Although we have previously revealed that ApoCIII serves as a type 1 diabetic serum factor, hyperactivating  $\beta$  cell  $\text{Ca}_V$  channels, only whole-cell patch-clamp analysis was performed [5]. Undoubtedly, detailed examination of biophysical properties of single  $\text{Ca}_V$  channels in ApoCIII-treated cells should be implemented to mechanistically dissect hyperactivation of  $\beta$  cell  $\text{Ca}_V$  channels by this apolipoprotein. Interestingly, cell-attached single channel recordings in the present work reveal that incubation with ApoCIII not only augments the activity of individual  $\beta$  cell  $\text{Ca}_V1$  channels but also enriches the number of functional  $\text{Ca}_V1$  channels in the recorded area of the  $\beta$  cell plasma membrane. The augmentation of single  $\text{Ca}_V1$  channel activity is visualized as an increased open probability attributed to the prolonged mean open time and shortened mean closed time. Enrichment of number of functional  $\text{Ca}_V1$  channels is verified by appearance of more levels of single  $\text{Ca}_V1$  channel conductance.

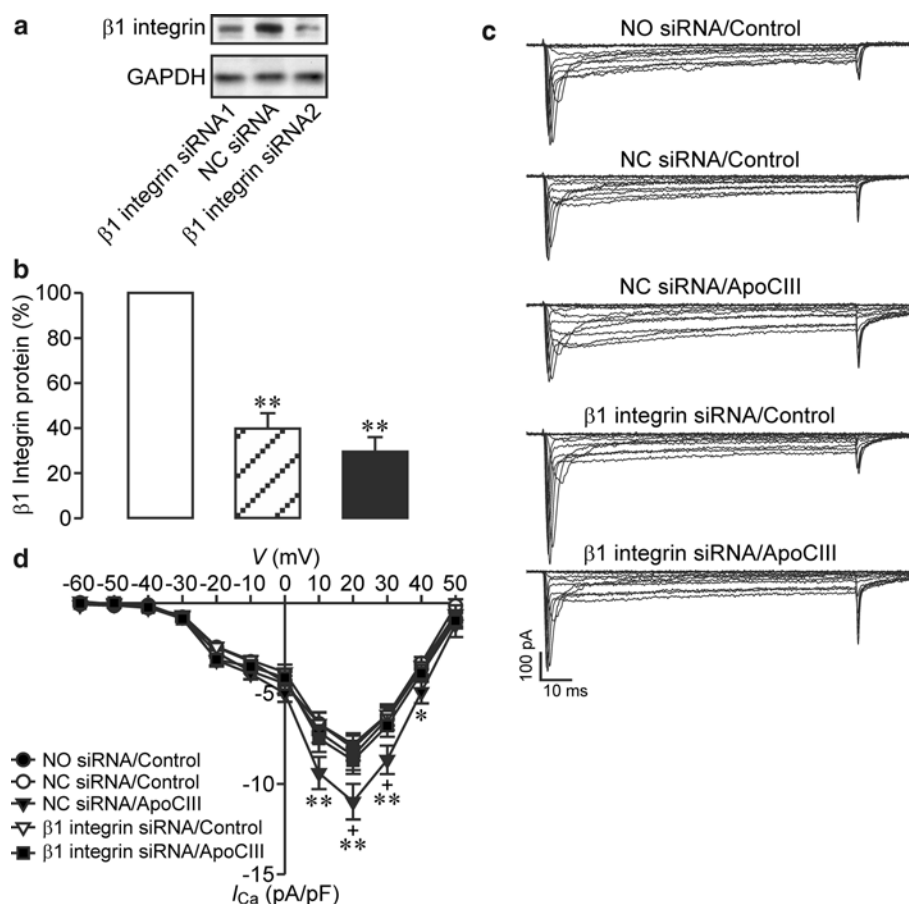


**Fig. 7** Knockdown of  $\beta 1$  integrin abrogates apolipoprotein CIII-induced exaggeration of whole-cell  $Ca^{2+}$  currents in RINm5F cells. **a** Representative blots of  $\beta 1$  integrin- and GAPDH-immunoreactive bands in  $\beta 1$  integrin siRNA #1-, negative control siRNA (NC siRNA)- and  $\beta 1$  integrin siRNA #2-transfected cells. **b** Immunoblot quantifications of  $\beta 1$  integrin protein in NC siRNA- (open column,  $n = 6$ ),  $\beta 1$  integrin siRNA #1- (hatched column,  $n = 6$ ) and  $\beta 1$  integrin siRNA #2-transfected RINm5F cells (filled column,  $n = 6$ ).  $**p < 0.01$  versus NC siRNA. **c** Sample whole-cell  $Ca^{2+}$  current traces registered in individual cells following mock transfection and incubation with control vehicle (NO siRNA/Control, cell capacitance: 12.1 pF), NC siRNA transfection and control vehicle treatment (NC siRNA/Control, cell capacitance: 11.4 pF), NC siRNA transfection and apolipo-

protein CIII (ApoCIII) incubation (NC siRNA/ApoCIII, cell capacitance: 12.1 pF),  $\beta 1$  integrin siRNA transfection and exposure to vehicle solution ( $\beta 1$  integrin siRNA/Control, cell capacitance: 11.9 pF) and  $\beta 1$  integrin siRNA transfection and ApoCIII exposure ( $\beta 1$  integrin siRNA/ApoCIII, cell capacitance: 12.4 pF), respectively. **d**  $Ca^{2+}$  current density–voltage relationships in cells subjected to NO siRNA/Control (filled circles,  $n = 29$ ), NC siRNA/Control (open circles,  $n = 28$ ), NC siRNA/ApoCIII (filled triangles,  $n = 28$ ),  $\beta 1$  integrin siRNA/Control (open triangles,  $n = 29$ ) and  $\beta 1$  integrin siRNA/ApoCIII (filled squares,  $n = 29$ ).  $*p < 0.05$  and  $**p < 0.01$  versus NO siRNA/Control, NC siRNA/Control and  $\beta 1$  integrin siRNA/Control.  $+p < 0.05$  versus  $\beta 1$  integrin siRNA/ApoCIII

The insulin-secreting RINm5F cell is equipped with  $Ca_v1$ ,  $Ca_v2$  and  $Ca_v3$  channels [1, 2]. We investigated if ApoCIII selectively hyperactivates  $Ca_v1$  channels or indiscriminately impacts all these three types of  $Ca_v$  channels in this insulin-secreting cell. It turned out that ApoCIII-induced hyperactivation of  $\beta$  cell  $Ca_v$  channels could no longer take place following pharmacological ablation of  $Ca_v1$  channels. This means that ApoCIII selectively hyperactivates  $Ca_v1$  channels, which are the major  $Ca_v$  channel type playing a predominant role over other types of  $Ca_v$  channels in  $\beta$  cell physiology and pathophysiology. Give that ApoCIII acts as the actual factor in type 1 diabetic serum to drive  $Ca^{2+}$ -dependent  $\beta$  cell death that

is prevented by the  $Ca_v1$  channel blocker verapamil, the selective hyperactivation of  $\beta$  cell  $Ca_v1$  channels observed in the present work most likely accounts for the pathophysiological role of this apolipoprotein in  $Ca^{2+}$ -dependent  $\beta$  cell [1, 2, 4, 5].

A series of protein kinases, such as PKA and PKC, can effectively phosphorylate  $Ca_v$  channels resulting in increases in the open channel density and activity due to phosphorylation-induced conformational changes in these channels [3, 28, 29]. Increases in the number and open probability of functional  $Ca_v$  channels by ApoCIII might be mediated by protein kinases. ApoCIII has been demonstrated to activate PKC through  $\beta 1$  integrin in monocytic

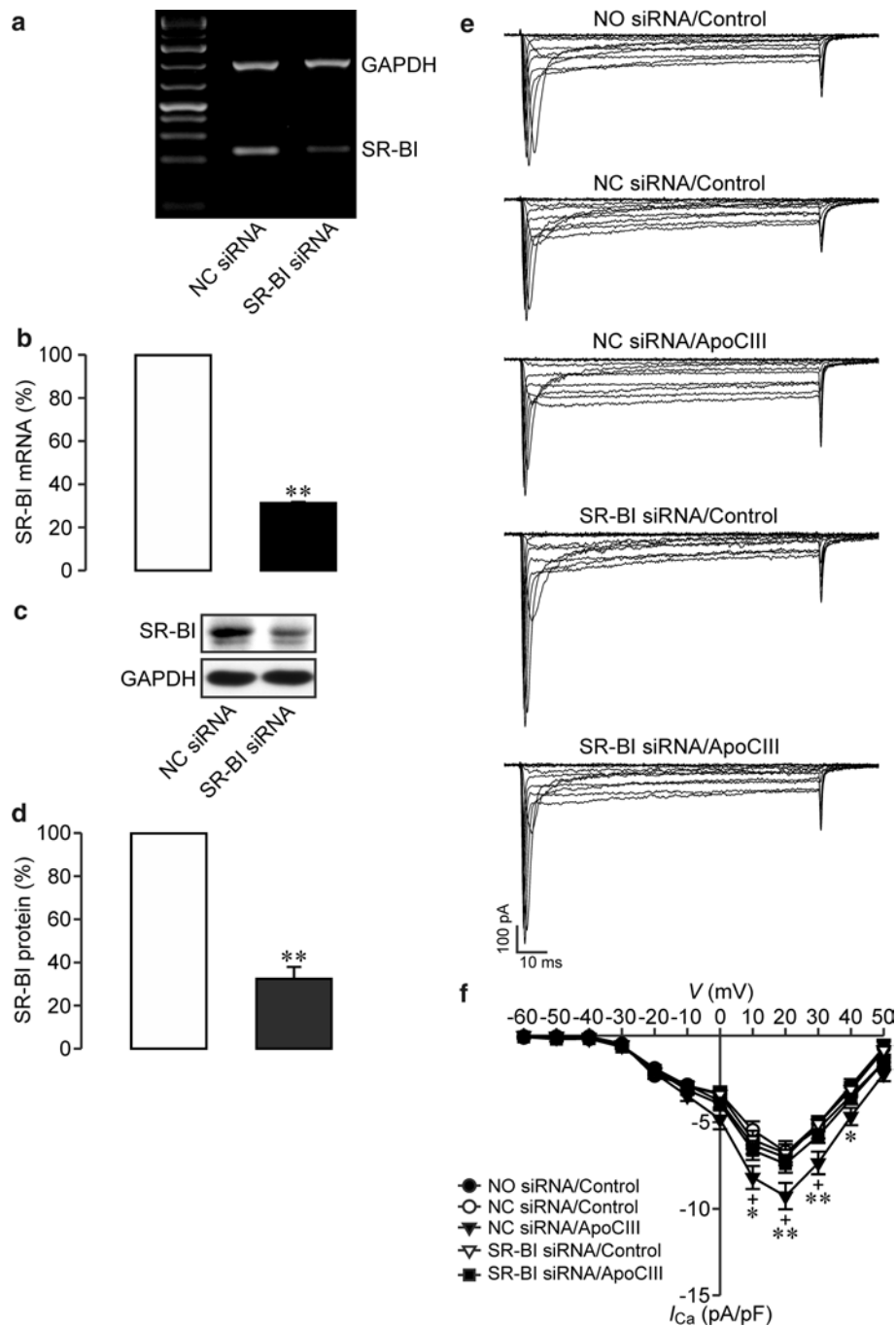


**Fig. 8** Knockdown of SR-BI prevents apolipoprotein CIII-induced enhancement of whole-cell  $Ca^{2+}$  currents in RINm5F cells. **a** Representative blots of GAPDH- and SR-BI-mRNA bands in negative control siRNA (NC siRNA)- and SR-BI siRNA-transfected cells. **b** Quantifications of SR-BI mRNA in NC siRNA- (*open column*,  $n = 7$ ) and SR-BI siRNA-transfected RINm5F cells (*filled column*,  $n = 7$ ).  $^{***}p < 0.01$  versus NC siRNA. **c** Sample blots of SR-BI- and GAPDH-immunoreactive bands in NC siRNA- and SR-BI siRNA-transfected cells. **d** Quantitative immunoblot measurements of SR-BI protein in NC siRNA- (*open column*,  $n = 7$ ) and SR-BI siRNA-transfected RINm5F cells (*filled column*,  $n = 7$ ).  $^{**}p < 0.01$  versus NC siRNA. **e** Representative whole-cell  $Ca^{2+}$  current traces from individual cells subsequent to mock transfection and incubation with control vehicle (NO siRNA/Control, cell capacitance: 13.87 pF), NC siRNA

transfection and control vehicle treatment (NC siRNA/Control, cell capacitance: 13.18 pF), NC siRNA transfection and apolipoprotein CIII (ApoCIII) incubation (NC siRNA/ApoCIII, cell capacitance: 13.53 pF), SR-BI siRNA transfection and exposure to vehicle solution (SR-BI siRNA/Control, cell capacitance: 12.90 pF) and SR-BI siRNA transfection and ApoCIII exposure (SR-BI siRNA/ApoCIII, cell capacitance: 13.01 pF), respectively. **f**  $Ca^{2+}$  current density–voltage relationships in cells subjected to NO siRNA/Control (*filled circles*,  $n = 30$ ), NC siRNA/Control (*open circles*,  $n = 29$ ), NC siRNA/apoCIII (*filled triangles*,  $n = 30$ ), SR-BI siRNA/Control (*open triangles*,  $n = 29$ ) and SR-BI siRNA/ApoCIII (*filled squares*,  $n = 30$ ).  $^{*}p < 0.05$  and  $^{**}p < 0.01$  versus NO siRNA/Control, NC siRNA/Control and SR-BI siRNA/Control.  $^{+}p < 0.05$  versus SR-BI siRNA/ApoCIII

cells [16]. Furthermore,  $\beta 1$  integrin activation can also upregulate  $\text{Ca}_v1$  channels in neurons, ventricular myocytes and vascular smooth muscle cells through stimulation of PKA, PKC and Src kinase [22–25]. All these components are present in  $\beta$  cells [2, 30–33] and may suggest that ApoCIII employs the  $\beta 1$  integrin-PKA/PKC/Src kinase cascade to hyperactivate  $\beta$  cell  $\text{Ca}_v$  channels. Indeed, the present work shows that complex inhibition of PKA, PKC and Src kinase effectively abrogates ApoCIII-induced hyperactivation of  $\beta$  cell  $\text{Ca}_v$  channels and that coinhibition of PKA and Src kinase is enough for this effect. However, individual inhibition of PKA, PKC or Src kinase only produced, if anything, a marginal effect on ApoCIII-induced hyperactivation of  $\beta$  cell  $\text{Ca}_v$  channels. Hence, we conclude that ApoCIII relies on parallel PKA and Src pathways to upregulate  $\beta$  cell  $\text{Ca}_v$  channels.

Occurrence of ApoCIII-induced hyperactivation of  $\beta$  cell  $\text{Ca}_v$  channels requires overnight incubation. Hence, the effect might be accounted for by an increase in  $\text{Ca}_v$  channel expression. Therefore, we quantified immunoreactivities of  $\text{Ca}_v1.2$  and  $\text{Ca}_v1.3$  subunits in RINm5F cells following overnight incubation with ApoCIII. However, the incubation had no influence on  $\beta$  cell  $\text{Ca}_v1$  channel expression. We therefore excluded the possibility that ApoCIII elevates  $\beta$  cell  $\text{Ca}_v1$  channel expression.

The transmembrane receptor  $\beta 1$  integrin is noncovalently associated with other integrins to form a set of heterodimers. They recognize a large number of soluble and surface-bound proteins to mediate cell–cell, cell–extracellular matrix and cell–pathogen interactions [34].  $\beta 1$  Integrin is situated downstream of ApoCIII and upstream of PKA/PKC/Src kinase in some cell types [16, 22–25]. This made us investigate whether the ApoCIII– $\beta 1$  integrin-PKA/PKC/Src kinase pathway operates in the  $\beta$  cell as the mechanism whereby this apolipoprotein hyperactivates  $\text{Ca}_v1$  channels. Interestingly, knockdown of  $\beta 1$  integrin does not influence  $\beta$  cell  $\text{Ca}_v$  channel activity in the absence of ApoCIII, but significantly abrogates ApoCIII-induced hyperactivation of  $\beta$  cell  $\text{Ca}_v$  channels. The results clearly verify that  $\beta 1$  integrin plays a significant role in mediating the action of ApoCIII on  $\beta$  cell  $\text{Ca}_v1$  channel activity.

Although  $\beta 1$  integrin can couple ApoCIII to the corresponding downstream effectors PKA, PKC and Src kinase,  $\beta 1$  integrin is unlikely to directly interact with this apolipoprotein [16, 22–25]. Previous work shows that SR-BI not only physically associates with ApoCIII but also interacts with  $\beta 1$  integrin [10, 26]. This pinpoints the possibility that SR-BI may serve as a molecular bridge between ApoCIII and  $\beta 1$  integrin with regard to  $\beta$  cell  $\text{Ca}_v$  channel hyperactivation. Indeed, in the present study we could demonstrate that SR-BI serves as a molecular bridge since SR-BI gene silencing efficiently nullifies ApoCIII-induced

hyperactivation of  $\beta$  cell  $\text{Ca}_v$  channels. This generates a complete picture of the novel cascade of  $\beta$  cell  $\text{Ca}_v$  channel hyperactivation, namely ApoCIII-SR-BI- $\beta 1$  integrin-PKA/Src.

It is worth noting that ApoCIII-induced hyperactivation of  $\beta$  cell  $\text{Ca}_v1$  channels observed in the present work occurred when cells were depolarized to more positive potentials than +10 mV. It seems that  $\beta$  cell  $\text{Ca}_v1$  channels in vivo never experience such strong depolarization and thus the effect of ApoCIII could hardly happen since the action potential of the  $\beta$  cell peaks at about –20 mV [35–37]. However, the effect of ApoCIII was detected by using the perforated whole-cell patch-clamp recording mode under experimental conditions where 10 mM  $\text{Ca}^{2+}$  was added in extracellular solution to obtain optimal  $\text{Ca}^{2+}$  currents. Such a high concentration of extracellular  $\text{Ca}^{2+}$  (10 mM) in comparison with physiological concentration of extracellular  $\text{Ca}^{2+}$  (2.5 mM) can significantly shift the I–V curve to more positive potentials [38–40]. The perforated whole-cell patch-clamp recording mode has a similar effect. Hence, under in vivo conditions ApoCIII is likely to affect  $\beta$  cell  $\text{Ca}_v1$  currents within the physiological membrane potential range [38–40].

In conclusion, our findings demonstrate that ApoCIII selectively hyperactivates  $\beta$  cell  $\text{Ca}_v1$  channels through parallel PKA and Src kinase pathways in a SR-BI/ $\beta 1$  integrin-dependent fashion. ApoCIII-induced hyperactivation of  $\beta$  cell  $\text{Ca}_v1$  channels is characterized by the enriched density and increased activity of functional  $\text{Ca}_v1$  channels in the  $\beta$  cell plasma membrane. Undoubtedly, this novel signal-transduction pathway has a potential to serve as an innovative drug discovery platform for the prevention of  $\text{Ca}^{2+}$ -dependent  $\beta$  cell death in association with diabetes.

**Acknowledgments** This work was supported by grants from Berth von Kantzow’s Foundation, Diabetes Research and Wellness Foundation, EuroDia (FP6-518153), the Family Erling-Persson Foundation, Fredrik and Ingrid Thuring’s Foundation, Funds of Karolinska Institutet, the Knut and Alice Wallenberg Foundation, Magn. Bergvall’s Foundation, Novo Nordisk Foundation, Skandia Insurance Company, Ltd., the Stichting af Jochnick Foundation, Strategic Research Program in Diabetes at Karolinska Institutet, the Swedish Alzheimer Association, the Swedish Diabetes Association, the Swedish Foundation for Strategic Research, the Swedish Research Council, the Swedish Society of Medicine, Torsten and Ragnar Söderberg Foundation, VIBRANT (FP7-228933-2) and Åke Wiberg’s Foundation. P.-O. Berggren is founder of the Biotech Company BioCrine AB and is also a member of the board of this company. S.-N. Yang is a consultant to BioCrine AB. BioCrine AB is developing ApoCIII as a novel druggable target for the treatment of diabetes.

## References

1. Yang SN, Berggren PO (2005)  $\beta$ -cell  $\text{Ca}_v$  channel regulation in physiology and pathophysiology. *Am J Physiol* 288:E16–E28

2. Yang SN, Berggren PO (2006) The role of voltage-gated calcium channels in pancreatic  $\beta$ -cell physiology and pathophysiology. *Endocr Rev* 27:621–676
3. Catterall WA (2000) Structure and regulation of voltage-gated  $\text{Ca}^{2+}$  channels. *Annu Rev Cell Dev Biol* 16:521–555
4. Juntti-Berggren L, Larsson O, Rorsman P, Ammala C, Bokvist K, Wahlander K, Nicotera P, Dypbukt J, Orrenius S, Hallberg A, Berggren PO (1993) Increased activity of L-type  $\text{Ca}^{2+}$  channels exposed to serum from patients with type I diabetes. *Science* 261:86–90
5. Juntti-Berggren L, Refai E, Appelskog I, Andersson M, Imreh G, Dekki N, Uhles S, Yu L, Griffiths WJ, Zaitsev S, Leibiger I, Yang SN, Olivecrona G, Jornvall H, Berggren PO (2004) Apolipoprotein CIII promotes  $\text{Ca}^{2+}$ -dependent  $\beta$  cell death in type 1 diabetes. *Proc Natl Acad Sci USA* 101:10090–10094
6. Sol EM, Sundsten T, Bergsten P (2009) Role of MAPK in apolipoprotein CIII-induced apoptosis in INS-1E cells. *Lipids Health Dis* 8:3
7. Holmberg R, Refai E, Höög A, Crooke RM, Graham M, Olivecrona G, Berggren PO, Juntti-Berggren L (2011) Lowering apolipoprotein CIII delays onset of type 1 diabetes. *Proc Natl Acad Sci USA* 108:10685–10689
8. Gangabadage CS, Zdunek J, Tessari M, Nilsson S, Olivecrona G, Wijmenga SS (2008) Structure and dynamics of human apolipoprotein CIII. *J Biol Chem* 283:17416–17427
9. Jong MC, Hofker MH, Havekes LM (1999) Role of ApoCs in lipoprotein metabolism: functional differences between ApoC1, ApoC2, and ApoC3. *Arterioscler Thromb Vasc Biol* 19:472–484
10. Xu S, Laccotripe M, Huang X, Rigotti A, Zannis VI, Krieger M (1997) Apolipoproteins of HDL can directly mediate binding to the scavenger receptor SR-BI, an HDL receptor that mediates selective lipid uptake. *J Lipid Res* 38:1289–1298
11. Clavey V, Lestavel-Delattre S, Copin C, Bard JM, Fruchart JC (1995) Modulation of lipoprotein B binding to the LDL receptor by exogenous lipids and apolipoproteins CI, CII, CIII, and E. *Arterioscler Thromb Vasc Biol* 15:963–971
12. Huard K, Bourgeois P, Rhoads D, Faltraut L, Cohn JS, Brissette L (2005) Apolipoproteins C-II and C-III inhibit selective uptake of low- and high-density lipoprotein cholesteryl esters in HepG2 cells. *Int J Biochem Cell Biol* 37:1308–1318
13. Chan DC, Watts GF, Redgrave TG, Mori TA, Barrett PH (2002) Apolipoprotein B-100 kinetics in visceral obesity: associations with plasma apolipoprotein C-III concentration. *Metabolism* 51:1041–1046
14. Sundsten T, Ostenson CG, Bergsten P (2008) Serum protein patterns in newly diagnosed type 2 diabetes mellitus—influence of diabetic environment and family history of diabetes. *Diabet Metab Res Rev* 24:148–154
15. Atzmon G, Rincon M, Schechter CB, Shuldiner AR, Lipton RB, Bergman A, Barzilai N (2006) Lipoprotein genotype and conserved pathway for exceptional longevity in humans. *PLoS Biol* 4:e113
16. Kawakami A, Aikawa M, Libby P, Alcaide P, Lusinskas FW, Sacks FM (2006) Apolipoprotein CIII in apolipoprotein B lipoproteins enhances the adhesion of human monocytic cells to endothelial cells. *Circulation* 113:691–700
17. Fang DZ, Liu BW (2000) Apolipoprotein C-III can specifically bind to hepatic plasma membranes. *Mol Cell Biochem* 207:57–64
18. Kawakami A, Aikawa M, Nitta N, Yoshida M, Libby P, Sacks FM (2007) Apolipoprotein CIII-induced THP-1 cell adhesion to endothelial cells involves pertussis toxin-sensitive G protein- and protein kinase C $\alpha$ -mediated nuclear factor- $\kappa$ B activation. *Arterioscler Thromb Vasc Biol* 27:219–225
19. Yang SN, Wenna ND, Yu J, Yang G, Qiu H, Yu L, Juntti-Berggren L, Kohler M, Berggren PO (2007) Glucose recruits  $\text{K}_{\text{ATP}}$  channels via non-insulin-containing dense-core granules. *Cell Metab* 6:217–228
20. Berggren PO, Yang SN, Murakami M, Efanov AM, Uhles S, Kohler M, Moede T, Fernstrom A, Appelskog IB, Aspinwall CA, Zaitsev SV, Larsson O, Moitoso de Vargas L, Fecher-Trost C, Weissgerber P, Ludwig A, Leibiger B, Juntti-Berggren L, Barker CJ, Gromada J, Freichel M, Leibiger IB, Flockerzi V (2004) Removal of  $\text{Ca}^{2+}$  channel  $\beta_3$  subunit enhances  $\text{Ca}^{2+}$  oscillation frequency and insulin exocytosis. *Cell* 119:273–284
21. Rorsman P, Arkhammar P, Berggren PO (1986) Voltage-activated  $\text{Na}^+$  currents and their suppression by phorbol ester in clonal insulin-producing RINm5F cells. *Am J Physiol* 251:C912–C919
22. Rueckschloss U, Isenberg G (2004) Contraction augments L-type  $\text{Ca}^{2+}$  currents in adherent guinea-pig cardiomyocytes. *J Physiol* 560:403–411
23. Waitkus-Edwards KR, Martinez-Lemus LA, Wu X, Trzeciakowski JP, Davis MJ, Davis GE, Meininger GA (2002)  $\alpha_4\beta_1$  Integrin activation of L-type calcium channels in vascular smooth muscle causes arteriole vasoconstriction. *Circ Res* 90:473–480
24. Wu X, Davis GE, Meininger GA, Wilson E, Davis MJ (2001) Regulation of the L-type calcium channel by  $\alpha_5\beta_1$  integrin requires signaling between focal adhesion proteins. *J Biol Chem* 276:30285–30292
25. Gui P, Wu X, Ling S, Stotz SC, Winkfein RJ, Wilson E, Davis GE, Braun AP, Zamponi GW, Davis MJ (2006) Integrin receptor activation triggers converging regulation of Cav1.2 calcium channels by c-Src and protein kinase A pathways. *J Biol Chem* 281:14015–14025
26. Bamberger ME, Harris ME, McDonald DR, Husemann J, Landreth GE (2003) A cell surface receptor complex for fibrillar beta-amyloid mediates microglial activation. *J Neurosci* 23:2665–2674
27. Ristic H, Srinivasan S, Hall KE, Sima AA, Wiley JW (1998) Serum from diabetic BB/W rats enhances calcium currents in primary sensory neurons. *J Neurophysiol* 80:1236–1244
28. Kavalali ET, Hwang KS, Plummer MR (1997) cAMP-dependent enhancement of dihydropyridine-sensitive calcium channel availability in hippocampal neurons. *J Neurosci* 17:5334–5348
29. Yang J, Tsien RW (1993) Enhancement of N- and L-type calcium channel currents by protein kinase C in frog sympathetic neurons. *Neuron* 10:127–136
30. Mukai E, Fujimoto S, Sato H, Oneyama C, Kominato R, Sato Y, Sasaki M, Nishi Y, Okada M, Inagaki N (2011) Exendin-4 suppresses Src activation and reactive oxygen species production in diabetic Goto-Kakizaki rat islets in an Epac-dependent manner. *Diabetes* 60:218–226
31. Kantengwa S, Baetens D, Sadoul K, Buck CA, Halban PA, Rouiller DG (1997) Identification and characterization of  $\alpha 3\beta 1$  integrin on primary and transformed rat islet cells. *Exp Cell Res* 237:394–402
32. Bosco D, Meda P, Halban PA, Rouiller DG (2000) Importance of cell-matrix interactions in rat islet  $\beta$ -cell secretion in vitro: role of  $\alpha 6\beta 1$  integrin. *Diabetes* 49:233–243
33. Nikolova G, Jabs N, Konstantinova I, Domogatskaya A, Tryggvason K, Sorokin L, Fassler R, Gu G, Gerber HP, Ferrara N, Melton DA, Lammert E (2006) The vascular basement membrane: a niche for insulin gene expression and  $\beta$  cell proliferation. *Dev Cell* 10:397–405
34. Luo BH, Carman CV, Springer TA (2007) Structural basis of integrin regulation and signaling. *Annu Rev Immunol* 25:619–647
35. Ashcroft FM, Rorsman P (1989) Electrophysiology of the pancreatic  $\beta$ -cell. *Prog Biophys Mol Biol* 54:87–143
36. Refai E, Dekki N, Yang SN, Imreh G, Cabrera O, Yu L, Yang G, Norgren S, Rossner SM, Inverardi L, Ricordi C, Olivecrona G, Andersson M, Jornvall H, Berggren PO, Juntti-Berggren L (2005) Transthyretin constitutes a functional component in pancreatic beta-cell stimulus-secretion coupling. *Proc Natl Acad Sci USA* 102:17020–17025

37. Yoon JC, Xu G, Deeney JT, Yang SN, Rhee J, Puigserver P, Levens AR, Yang R, Zhang CY, Lowell BB, Berggren PO, Newgard CB, Bonner-Weir S, Weir G, Spiegelman BM (2003) Suppression of beta cell energy metabolism and insulin release by PGC-1alpha. *Dev Cell* 5:73–83
38. Byerly L, Chase PB, Stimers JR (1985) Permeation and interaction of divalent cations in calcium channels of snail neurons. *J Gen Physiol* 85:491–518
39. Green WN, Andersen OS (1991) Surface charges and ion channel function. *Annu Rev Physiol* 53:341–359
40. Ganitkevich V, Shuba MF, Smirnov SV (1988) Saturation of calcium channels in single isolated smooth muscle cells of guinea-pig taenia caeci. *J Physiol* 399:419–436